Polarized deuteron elastic scattering at 79 MeV and the effects of breakup channel coupling

E. J. Stephenson, J. C. Collins, C. C. Foster, D. L. Friesel, W. W. Jacobs, W. P. Jones, M. D. Kaitchuck, and P. Schwandt
Indiana University Cyclotron Facility, Bloomington, Indiana 47405

W. W. Daehnick
University of Pittsburgh, Pittsburgh, Pennsylvania 15260
(Received 12 November 1982)

We report angular distribution measurements of the cross section, the vector analyzing power (A_y), and two tensor analyzing powers [A_{yy} and $X_2=(2A_{xx}+A_{yy})/\sqrt{3}$] for the elastic scattering of 79-MeV polarized deuterons from ^{58}Ni. These measurements are compared in detail with folding model calculations that include perturbative corrections for coupling to deuteron breakup channels.

[NUCLEAR REACTIONS ^{58}Ni($\vec{d}$,d), $E_d=79$ MeV, measured elastic $\sigma(\theta)$, and analyzing powers $A_y(\theta)$, $A_{yy}(\theta)$, and $X_2=[2A_{xx}(\theta)+A_{yy}(\theta)]/\sqrt{3}$; comparison with folding and breakup coupled-channel models.]

I. INTRODUCTION

One objective of an analysis of deuteron elastic scattering is to obtain a good quantitative description of the measurements in terms of the interaction of the individual proton and neutron with the target nucleus. Within the context of a local optical model, a simple approach to this problem is to use folding, where the neutron and proton phenomenological optical potentials determined at half the deuteron bombarding energy are averaged over the free space deuteron internal wave function. This approach, first suggested by Watanabe,[1] gives central and vector spin-orbit deuteron potentials with about double the strength of the corresponding single nucleon potentials, but with a greater surface diffusivity which arises from averaging over the deuteron wave function. This model has been extended[2] to include the deuteron D state, with the chief result that a complex tensor potential was added to the deuteron optical model. Usually designated by T_R, this tensor potential depends quadratically on the scalar product of the deuteron spin vector with the deuteron-nucleus radius vector. The predictions generated from the folding model are generally at variance with elastic scattering measurements,[3] and as a result have been used only as a guide for obtaining phenomenological deuteron optical potentials.

In this paper we present new measurements of the cross section and three analyzing powers, the vector (A_y) and two tensors (A_{yy} and X_2), for 79-MeV deuteron elastic scattering from ^{58}Ni. We compare these data with calculations by Rawitscher and Mukherjee[4] that are based on the folding model. These calculations include a perturbative correction for coupling to the deuteron breakup channels.

Unlike the cross sections at lower bombarding energies, the 79-MeV data exhibit an enhancement near 60° due to the appearance of rainbow scattering.[5] This process leads to vector and A_{yy} tensor analyzing power angular distributions that become less diffractive and saturate near unity for large scattering angles. This phenomenon is largely an effect of just the real potential,[5] unlike the diffractive angular distributions at forward angles. Thus elastic scattering measurements near the rainbow angle may be sensitive in new ways to the theoretical calculations. For this reason, we have extended the angular distribution measurements to large scattering angles ($\theta<112°$) so that any new features will be readily apparent. Preliminary versions of parts of this data have appeared elsewhere.[4–9]

Hooten and Johnson have pointed out that the X_2 tensor analyzing power is free to first order of contributions from the deuteron spin-orbit potential.[10] Because of the large spin-orbit effects due to rainbow scattering,[5] a measurement of X_2 was made to obtain some information on the tensor terms, such as T_R, in the deuteron-nucleus optical potential.

In Sec. II we review the features of the experiment, and in Sec. III compare our measurements to the model. A summary and final remarks are given in Sec. IV.

II. EXPERIMENT

We have studied the spin dependence of deuteron elastic scattering from a ^{58}Ni target. Angular distribution measurements were made for the differential cross section, $\sigma(\theta)$, and three analyzing powers, $A_y(\theta)$, $A_{yy}(\theta)$, and the combination

$$X_2(\theta)=(2A_{xx}+A_{yy})/\sqrt{3}\ ,$$

between the center-of-mass scattering angles of 8° and 112°. These data were accumulated over six running periods for which the beam energy, as determined by magnetic analysis, ranged from 78.7 to 79.7 MeV.

The polarized deuteron beam was generated in an atomic beam source equipped with three atomic rf transition cavities, providing either pure vector or a combination of vector and tensor polarized beams with either sign of polarization. A review of the operation of this type of ion source and its rf transition cavities may be found in Ref. 11. The spin states of the beam were controlled remotely, and changed periodically (about twice per minute) during

each data acquisition run in order to reduce systematic errors arising from slowly-varying experimental parameters (e.g., beam spot position, electronic thresholds, etc.).

The beam polarization was measured between the data acquisition runs by inserting a target gas cell containing ^{3}He into the beam line between the injector and main cyclotrons where the deuteron beam energy (after degradation in the gas cell walls) was 7.1 MeV. Protons from the ^{3}He($\vec{d}$,p)^{4}He reaction were detected with plastic scintillation counters at 67° to the left and right of the beam. The beam was centered dynamically on collimating slits immediately preceding the gas cell, and the amount of beam transmitted through the slits was measured in a Faraday cup immediately behind the gas cell.

The low-energy polarimeter was calibrated using the ^{16}O($\vec{d}$,α)^{14}N* reaction leading to the 0^+ state of ^{14}N at 2.31 MeV. Because both initial and final nuclei have spin and parity 0^+, the scattering matrix elements are constrained such that $A_{yy} = -2$, independent of scattering angle and bombarding energy.[12] This calibration was transferred to the A_{yy} measured in the ^{3}He($\vec{d}$,p)^{4}He reaction with a relative error of about 3%. The major contribution to the uncertainty in this calibration arose from the effects of beam polarization moments other than A_{yy} (such as A_{xx}-A_{zz}) to which the ^{3}He($\vec{d}$,p)^{4}He reaction is sensitive and the ^{16}O($\vec{d}$,α)^{14}N reaction is not. By adjusting the polarimeter vector analyzing power, a value could be found that made the vector and tensor beam polarizations for each transition a consistent fraction of their maximum values. Such a calibration procedure assumes that any depolarizing mechanism affects all moments equally. The analyzing powers so obtained ($A'_y = -0.292$ and $A'_{yy} = -0.839$) agree with a smooth interpolation in energy through the ^{3}He($\vec{d}$,p)^{4}He measurements of Grüebler *et al.*[13] However, beam polarization measurements based on the published analyzing powers for ^{3}He($\vec{d}$,p)^{4}He at other angles[13] or for ^{4}He($\vec{d}$,d)^{4}He elastic scattering[14] give values inconsistent with those obtained here by as much as 40%. These discrepancies created significant normalization errors in preliminary vector analyzing power measurements reported from the Indiana University Cyclotron Facility (IUCF). The A_y values published in Ref. 4 must be multiplied by 0.747 to agree with the measurements reported here.

The beam polarization in each spin state was measured relative to the unpolarized state using the formulas

$$p_y = \frac{I_u}{3 I_p A'_y}\left[\frac{C_{pl}}{C_{ul}} - \frac{C_{pr}}{C_{ur}}\right],$$
$$p_{yy} = \frac{1}{A'_{yy}}\left[\frac{I_u}{I_p}\left[\frac{C_{pl}}{C_{ul}} + \frac{C_{pr}}{C_{ur}}\right] - 2\right], \quad (1)$$

where the $C_{\alpha\beta}$ are the dead time corrected count rates for the α polarization state (either polarized or unpolarized) and the β detector (either left or right). The I_α are the integrated beam currents for each polarization state; A'_y and A'_{yy} are, respectively, the vector and tensor analyzing powers for the polarimeter. The beam polarization varied between 85% and 89% of the maximum possible polarization for each state. Measurements of the residual beam current obtained with the ion source sextupole magnet valved off from the ionizer suggest that over half of the observed depolarization results from the ionization of background gas. Each rf transition unit was adjusted in magnetic field strength and frequency to establish that its operation was maximally efficient. The polarization of the beam was constant with time for each experimental setup, hence the time-averaged values were used for computing the analyzing powers in $\vec{d}+^{58}$Ni elastic scattering. This procedure assumes that the polarization measured with the low-energy polarimeter is maintained throughout the acceleration process in the main cyclotron and subsequent beam transport. The meaurements reported in this paper set an upper limit of about 8% on any depolarizing effects. Conversely, an increase in beam polarization through the selection of the low-emittance portions of the beam during acceleration cannot be ruled out, although this effect is expected to be small for an atomic beam source. Because the elastic scattering analyzing powers are large and can be precisely measured at 80 MeV, a useful analyzing power standard measured to high precision is needed at these energies.

The targets used in this experiment were 99.93% isotopically enriched ^{58}Ni. They were made by rolling metallic nickel. Their thicknesses ranged from 8.3 to 150 mg/cm^2, and were determined by weighing samples of the rolled foils. Comparisons among cross sections measured with targets of different thickness gave values consistent to within 5%. All cross sections were normalized to the value obtained when the 28.5 mg/cm^2 target was mounted perpendicular to the beam. Variations introduced by rotating the targets to accommodate larger scattering angles were small. The corrections were obtained by repeating cross section measurements at the same angle for a number of target positions.

Measurements at laboratory angles less than 50° were made with a Faraday cup mounted inside the scattering chamber. Backscattered electrons were suppressed with a magnet mounted in front of the cup. This cup was split into left and right halves. During data acquisition, the horizontal location of the beam spot was held fixed by automatically correcting the horizontal beam steering based on currents read by the two halves of the Faraday cup. Small adjustments were made in the horizontal cup position at the start of each running period to ensure that the beam passed through the target at the center-of-rotation of the magnetic spectrometer.

In order to decrease room background for the measurements at large scattering angle, a second beam dump was located in the shielded wall far behind the target chamber. For the thicker (or rotated) targets, there were significant multiple-scattering losses as the beam travelled to the Faraday cup. Again, corrections were made for each target and target-angle combination by remeasuring cross sections with targets of smaller effective thickness. All cross sections were normalized to the values obtained using the Faraday cup mounted inside the scattering chamber. The total normalization error in the absolute cross section is estimated to be 10%. From angle to angle, the variations due to systematic errors are likely to be less than 5%.

Measurements of the cross section, vector analyzing power, and A_{yy} tensor analyzing power were made by detecting scattered deuterons in the QDDM magnetic

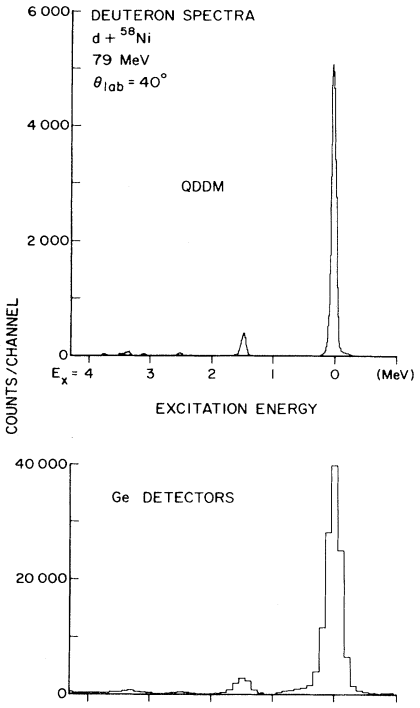

FIG. 1. Energy spectra for deuterons scattered from ^{58}Ni at a laboratory angle of 40°. The top part of the figure is a position spectrum from the focal plane of the QDDM magnetic spectrometer. The bottom part is a pulse height spectrum obtained with a silicon and high-purity germanium detector telescope.

spectrometer. The spectrometer entrance slits, a distance of 0.47 m from the target, were adjusted to provide solid angles between 0.19 and 1.08 msr. This variation provided a scattering angle acceptance ranging from 0.45° at forward angles to 1.03° at large angles. The particles were identified as deuterons on the basis of energy-loss signals from two plastic scintillation detectors mounted behind the focal plane. The focal plane position of each particle was measured with a proportional counter wire chamber, which was read by measuring the relative time of arrival of signals at either end of the helical cathode delay line. A sample position spectrum, shown in the top part of Fig. 1, has a FWHM resolution of about 100 keV.

Variations in the tuning of the beam among the different running periods produced changes in the angle of the beam incident on the target. The absolute scattering angle setting of the QDDM was determined by comparing cross section measurements made with the spectrometer on either side of the beam near the 20° cross section minimum. Variations in the angle of incidence among different running periods were as large as 0.3°. The absolute scattering angle is known from this procedure to less than 0.1°. During this procedure, the horizontal location of the beam spot was held fixed by the signals from the split Faraday cup.

Dead-time corrections were determined using a pulser triggered at a rate proportional to the beam current, as determined by the beam integrator. The pulser signals were fed into the focal plane electronic circuits and analyzed in the computer along with the data from real events. The accumulated pulser counts in a computer-generated spectrum were compared with the number of times the pulser was triggered during each run to compute the dead time. Dead times were less than 10%, and were dominated by conversion and readout times at the computer interface.

Elastic-scattering cross sections were measured at each angle for five deuteron beam spin states, including unpolarized (unp), vector polarized ($V+$ and $V-$), and tensor polarized ($T+$ and $T-$) beams. The counting times for each spin state were approximately equal. For each spin state, the experimental quantity of interest was the yield, Y, which is the ratio of the elastic scattering count rate (corrected for dead time) to the total charge indicated by the beam integration circuit. From Eq. (1), the vector and tensor beam polarizations were known for each spin state. An iterative scheme was employed to calculate the analyzing powers. To first approximation,

$$A_y = \frac{2[Y(V+)-Y(V-)]}{3[p_y(V+)-p_y(V-)]Y(\text{unp})} ,$$
$$A_{yy} = \frac{2[Y(T+)-Y(T-)]}{[p_{yy}(T+)-p_{yy}(T-)]Y(\text{unp})} , \tag{2}$$

where the p's refer to the beam polarization for various spin states. Other beam polarization components influence these calculations, and the lowest order correction is

$$A_y \leftarrow A_y - \frac{A_{yy}[p_{yy}(V+)-p_{yy}(V-)]}{3[p_y(V+)-p_y(V-)]} ,$$
$$A_{yy} \leftarrow A_{yy} - \frac{3A_y[p_y(T+)-p_y(T-)]}{[p_{yy}(T+)-p_{yy}(T-)]} . \tag{3}$$

In all cases, these corrections were less than ±0.02.

The statistical errors in the analyzing powers are quite small, with most errors falling in the range from 0.001 to 0.016 for A_y and 0.004 to 0.020 for A_{yy}. Perhaps the best estimate of the systematic errors comes from measurements at overlapping or closely-spaced angles. The scatter of data points suggests a systematic relative error less than 0.02, except at angles smaller than 15°, where it may be as large as 0.03. The statistical error in the average beam polarization was less than 0.013, and usually did not make the largest contribution to the error in the analyzing power. As mentioned earlier, there is a normalization error of 3% from the calibration of the polarimeter and an unknown normalization error due to the transmission of that polarization through the cyclotron.

As pointed out by Perrin *et al.*,[15] a measurement of the quantity

$$X_2 = (2A_{xx} + A_{yy})/\sqrt{3}$$

can be carried out with a p_{yy} tensor polarized beam provided that the scattering plane is at an angle of 54.7° to the horizontal (or xz) plane. At that angle, the polarized cross section depends on the moments of the beam according to

$$\sigma = \sigma_0[1 + \sqrt{3}p_y A_y/2 + p_{yy}X_2/(2\sqrt{3})] . \tag{4}$$

Measurements of X_2 were carried out with a solid-state counter telescope mounted on a rotating platform at

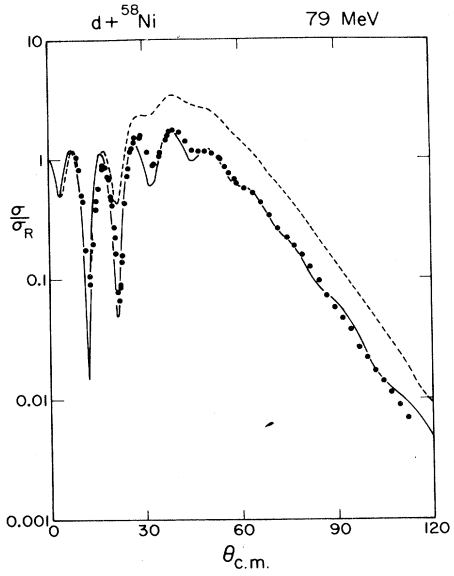

FIG. 2. Angular distribution of the ratio of the measured cross section to the Rutherford cross section for deuteron elastic scattering from ^{58}Ni. The curves are calculations based on the folding model that either do (solid) or do not (dashed) include coupling to deuteron breakup channels.

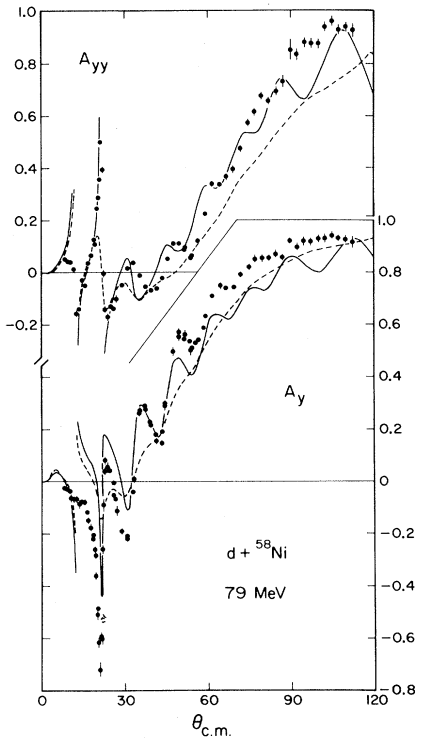

FIG. 3. Angular distributions of the A_{yy} and A_y analyzing powers for deuteron elastic scattering from ^{58}Ni. The curves are described in the caption to Fig. 2.

54.7°±0.4° to the horizontal plane. The angle uncertainty combines geometric errors and uncertainties due to motion of the beam on target. The detector telescope consisted of a 2-mm thick silicon surface-barrier transmission detector followed by a 15-mm high-purity germanium detector[16] cooled by liquid nitrogen. The scattered particles were collimated by a circular aperture 20 mm in diameter at a distance of 368 mm from the target ($\Omega=0.59$ msr). For an event to be valid, both detectors were required to generate a pulse within a resolving time of 250 ns. The total energy was taken as the analog sum of the detector outputs, with coefficients scaled for the difference in ionization potential between silicon and germanium. The resolution of this system was degraded because the beam just before the target and the scattered particles travelled through air. A sample spectrum with a FWHM resolution of 260 keV is shown in the bottom part of Fig. 1.

Because of the low count rate (reduced to minimize electronic pileup from the large singles count rate) and the small coefficients in Eq. (4), the statistical precision of the X_2 measurements was worse than for the other analyzing powers. The statistical errors ranged from 0.009 to 0.100. However, systematic errors may be worse because there was no position stabilization of the beam spot on target and because geometric constraints prevented us from determining an absolute scattering angle.

The cross section and analyzing power angular distributions are shown in Figs. 2–4 with statistical errors only. Tables of the measurements are available on request from the authors. The distributions show diffractive oscillations at all angles. At large angles these oscillations are damped. The cross section then falls exponentially, while A_y and A_{yy} rise to almost unity. The measured values of X_2 are near zero at all angles. These general features are consistent with the rainbow scattering picture, and have been described in detail elsewhere.[5]

III. COUPLING OF ELASTIC SCATTERING TO THE BREAKUP CONTINUUM

Recently calculations have become available in which the elastic deuteron channel, including the spin degrees of freedom, is coupled to the deuteron breakup continuum.[4]

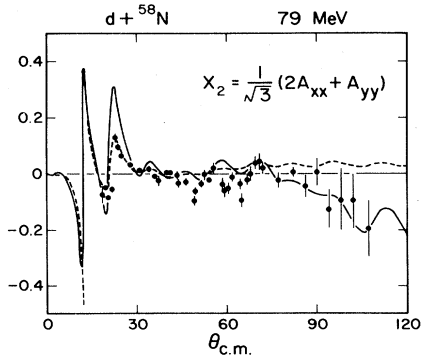

FIG. 4. Angular distribution of the $X_2=(2A_{xx}+A_{yy})/\sqrt{3}$ tensor analyzing power. The curves are described in the caption to Fig. 2.

The breakup channels have been estimated to comprise about 28% of the reaction cross section at 80 MeV. If their effect is nearly coherent, they would form the most important reaction channel to consider for coupling to elastic scattering. We will review briefly the main features of this calculation and compare the results to our measurements.

For this calculation,[4] a folding model is used to construct the complex central and vector spin-orbit potentials for the deuteron. The nucleon-nucleus potentials are obtained from optical model analyses made near 40 MeV bombarding energy.[17] From these folded potentials, a first calculation is made of the elastic scattering wave function. The effects of the deuteron D state, as expressed through the folding-model complex T_R potential,[2] are included as a perturbation in the calculation of the second-order scattering matrix elements. A set of deuteron breakup states is chosen to represent S- and D-wave relative n-p angular momenta, a discretized relative n-p momentum, and no nuclear excitation. These states couple to elastic scattering through gradients in the optical potential. The breakup wave functions are calculated, and their influence on the elastic scattering matrix is also treated as a perturbation.

Figures 2–4 show the measurements along with the folding-model calculation (dashed line, including the effects of the T_R potential) and the coupled-channel calculation (solid line). These calculations shown here differ from those presented in Ref. 4 in that they contain 42 partial waves, 10 more than previously considered. This change substantially reduces spurious oscillations at large scattering angles in the calculation.

Given that there are no adjustable features in the model aside from ambiguities in the optical model input (neither the choice of momentum bins for the continuum nor the angular momentum cutoff at $l=2$ appears to be a restrictive approximation), the agreement with the cross section and analyzing power angular distributions is remarkably good. The inclusion of coupling to the breakup channel is clearly important, producing a factor of 2 change in the cross section at all angles past 30°. This change produces good agreement with the cross section beyond 15°. The analyzing powers show an increase in the size of the diffractive oscillations, which improves the agreement with A_y and A_{yy} at angles between 20° and 60°. An increase in the magnitude of A_{yy} also helps the quality of the agreement.

At more forward angles, the major discrepancies are related in part to the diffraction minima in the cross section. The minimum near 10° is too deep, and the oscillations in the analyzing powers at those angles are too large. These difficulties are typical of similar calculations at lower bombarding energies.[4] It thus appears that these coupled-channel calculations are considerably better near the rainbow angle where the effects of the real optical potential dominate.

The values of X_2 have maximum magnitudes about half those observed at lower energies.[18] In part, this may arise from the action of the spin-orbit potential. As A_y approaches unity (an effect of rainbow scattering), X_2 must approach zero.[12] The calculation suggests that a T_R potential plus tensorlike effects from breakup coupling do not disturb this behavior. The calculation gives values of

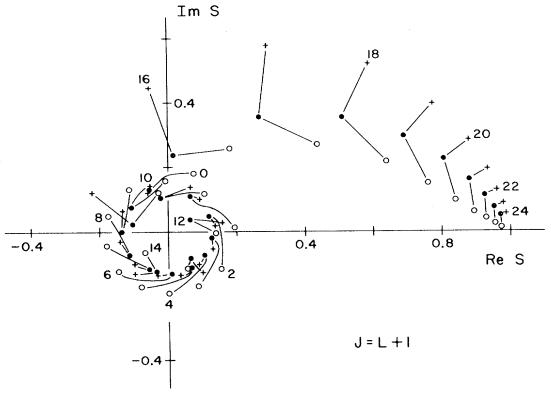

FIG. 5. Comparison of the S-matrix values with $J=L+1$ for deuteron elastic scattering from ^{58}Ni at 79 MeV. The values come from folding model calculations that either do (solid dots) or do not (crosses) include coupling to deuteron breakup channels, and from a phenomenological optical potential (open points). Lines connect S-matrix values that correspond to the same value of L.

X_2 small in magnitude and becoming more negative at angles beyond 30°, in qualitative agreement with the measurements. Perhaps more importantly, this calculation for X_2 does not suggest that there is any major problem with the folding-model T_R potential. This conclusion is quite different if a phenomenological optical potential with no breakup channel coupling is employed.[5] Then even a much smaller real T_R potential generates large values of X_2, and the imaginary T_R potential substantially reduces the large-angle values of A_y and A_{yy}. To remain close to the measurements, the strength of a T_R potential in the phenomenological optical potential model must be at least a factor of 10 smaller.

A phenomenological optical model containing only a complex central and real spin-orbit potential provides satisfactory agreement with the measurements.[19] Thus it may be helpful to compare the values of the S-matrix elements of the phenomenological optical model with those from the coupled-channel calculation as a way of assessing the quality of the approximations, especially the use of a perturbative method. The agreement is not expected to be exact since the coupled-channel calculation explicitly includes a nonlocal effect that is beyond the scope of the local optical potential. Figure 5 shows the scattering matrix elements (for the case where $J=L+1$) for the folding model and coupled-channel calculations, as well as those from the phenomenological model. To facilitate comparison, the three calculations for each L value are connected by lines. At large L values, the coupled-channel calculation moves from the folding model toward the phenomenological elements, but with an offset of one unit of L. The resulting S-matrix elements have about the right magnitude, but there are changes in phase. A similar effect is noted at lower energies, where this discrepancy is corrected to a large extent by replacing the perturbation theory with full channel coupling.[4] Unfortunately, a fully

coupled calculation has not been carried out with all spin degrees of freedom included. At moderate values of L (near $L=0$), the perturbative calculation moves the matrix elements away from both the folding model and phenomenological ones. At low L values, almost no change is seen when channel coupling is included. These discrepancies may arise for small L values because other mechanisms, such as Pauli exclusion, contribute to deuteron breakup. This calculation includes only those contributions due to the gradient of the potential at the nuclear surface.

For the future, it will be important to assess the validity of the perturbation theory approach in the case where spin is explicitly included. Calculations without spin suggest that the first-order perturbation calculation overestimates the effects of breakup in the total cross section. A full coupled-channel calculation gives a total breakup cross section that is a factor of 3 smaller than that obtained using first-order perturbation theory.[20] At present, there is good agreement between the estimate of the total breakup cross section from the perturbation theory calculation and measurements[21] of inclusive proton spectra from deuteron bombardment of ^{58}Ni. However, this calculation does not include several possible contributions to the breakup process, including the effects of Pauli exclusion, the Coulomb field of the nucleus, and nuclear excitation. Inelastic breakup processes, shown in other calculations to be the dominant form of breakup,[22] are included here only through the absorptive parts of the proton and neutron optical potentials.

IV. SUMMARY OF RESULTS AND FUTURE PROSPECTS

As a result of the series of experiments discussed in this paper, angular distribution measurements of the cross section and three analyzing powers are now available for the elastic scattering of 79-MeV deuterons from ^{58}Ni to large scattering angles. These data agree with the rainbow picture, namely that an enhancement in the large-angle elastic cross section is associated with a damping of the diffractive oscillations and the rise of both A_y and A_{yy} to almost unity at large scattering angles. The measurements of X_2, which are expected to be free of first-order contributions from the spin-orbit potential, are nearly zero at all angles. For theories of deuteron-nucleus scattering, rainbow scattering provides a regime, distinct from that dominated by diffractive scattering, where the theoretical predictions may be tested in new ways. Because the large-angle scattering is dominated by one spin state, it is expected that a consideration of spin is crucial even to obtain valid estimates of the cross section.

The simplest microscopic theory of deuteron-nucleus scattering, namely the folding model, has been improved by the calculation of corrections for coupling to breakup channels, including the effects of deuteron spin. The calculation of Rawitscher and Mukherjee estimates the effects of coupling to deuteron breakup channels through a first-order perturbation theory. This correction generates remarkable agreement with the cross section and all measured analyzing powers. The agreement is generally better near the rainbow angle where the scattering process is sensitive almost exclusively to the real part of the interaction. Unlike the conclusions obtained with phenomenological optical models alone, this channel-coupling calculation does not suggest that there is any difficulty with including the full strength T_R potential that arises from the deuteron D state.

These breakup calculations need to be repeated with full channel coupling so that the validity of the perturbation theory may be assessed. The clear suggestion from calculations without spin is that the correction will be reduced, thus causing the calculated values to retreat from the measurements, leaving a gap that could possibly be closed by other effects.

At these higher energies, the folding model appears to be a good starting point for considering the effects of deuteron breakup on deuteron elastic scattering. It can also serve as a reference for calculations that antisymmetrize the deuteron wave function in the field of the nucleus, contain relativistic modifications to the deuteron scattering wave function, or consider the effects of various nonlocalities. Such a common basis will be helpful in comparing and synthesizing the evaluation of various corrections. In the future, it may be necessary to compare these corrections to more complete sets of measurements, including A_{xz} and the breakup cross section and analyzing powers.

[1]S. Watanabe, Nucl. Phys. 8, 484 (1958).
[2]G. R. Satchler, Nucl. Phys. 21, 116 (1960); J. Raynal, Centre d'Etudes Nucleaires de Saclay Report No. CEA-R2511, 1965.
[3]P. W. Keaton, Jr. and D. D. Armstrong, Phys. Rev. C 8, 1692 (1973).
[4]G. H. Rawitscher and S. N. Mukherjee, Nucl. Phys. A342, 90 (1980).
[5]E. J. Stephenson, C. C. Foster, P. Schwandt, and D. A. Goldberg, Nucl. Phys. A359, 316 (1981).
[6]W. W. Daehnick, J. D. Childs, and Z. Vrcelj, Phys. Rev. C 21, 2253 (1980).
[7]W. W. Daehnick, in *Polarization Phenomena in Nuclear Physics—1980 (Fifth International Symposium, Santa Fe)*, Proceedings of the Fifth International Symposium on Polarization Phenomena in Nuclear Physics, AIP Conf. Proc. No. 69, edited by G. G. Ohlson, R. E. Brown, N. Jarmie, M. W. McNaughton, and G. M. Hale (AIP, New York, 1981), p. 487.
[8]E. J. Stephenson, J. C. Collins, C. C. Foster, D. L. Friesel, J. R. Hall, W. W. Jacobs, W. P. Jones, S. Kailas, M. Kaitchuck, P. Schwandt, W. W. Daehnick, and D. A. Goldberg, in *Polarization Phenomena in Nuclear Physics—1980 (Fifth International Symposium, Santa Fe)*, Proceedings of the Fifth International Symposium on Polarization Phenomena in Nuclear Physics, AIP Conf. Proc. No. 69, edited by G. G. Ohlson, R. E. Brown, N. Jarmie, M. W. McNaughton, and G. M. Hale (AIP, New York, 1981), p. 484.
[9]J. R. Shepard, E. Rost, and D. Murdock, Phys. Rev. Lett. 49, 14 (1982).
[10]D. J. Hooten and R. C. Johnson, Nucl. Phys. A175, 583 (1971); R. C. Johnson, *ibid.* A293, 92 (1977).

[11]W. Haeberli, Annu. Rev. Nucl. Sci. 17, 373 (1967).
[12]F. Seiler, F. N. Rad, H. E. Conzett, and R. Roy, Nucl. Phys. A296, 205 (1978), and references therein.
[13]W. Grüebler, V. König, A. Ruh, P. A. Schmelzbach, R. E. White, and P. Marmier, Nucl. Phys. A176, 631 (1971).
[14]W. Grüebler, V. König, P. A. Schmelzbach, and P. Marmier, Nucl. Phys. A134, 686 (1969); V. König, W. Grüebler, P. A. Schmelzbach, and P. Marmier, *ibid.* A148, 380 (1970); W. Grüebler, V. König, P. A. Schmelzbach, and P. Marmier, *ibid.* A148, 391 (1970), with recalibrations reported in V. König, W. Grüebler, A. Ruh, R. E. White, P. A. Schmelzbach, R. Risler, and P. Marmier, *ibid.* A166, 393 (1971), and W. Grüebler, P. A. Schmelzbach, V. König, R. Risler, and D. Boerma, *ibid.* A242, 265 (1975).
[15]G. Perrin, Nguyen Van Sen, J. Arvieux, R. Darves-Blanc, J. L. Durand, A. Fiore, J. C. Gondrand, F. Merchez, and C. Perrin, Nucl. Phys. A282, 221 (1977).
[16]D. L. Friesel, R. Pehl, and B. Flanders (unpublished).
[17]F. D. Becchetti, Jr. and G. W. Greenlees, Phys. Rev. 182, 1190 (1969).
[18]K. Hatanaka, M. Nakamura, K. Imai, T. Noro, H. Shimizu, H. Sakamoto, J. Shirai, T. Matsusue, and K. Nisimura, in *Polarization Phenomena in Nuclear Physics—1980 (Fifth International Symposium, Santa Fe),* Proceedings of the Fifth International Symposium on Polarization Phenomena in Nuclear Physics, AIP Conf. Proc. No. 69, edited by G. G. Ohlson, R. E. Brown, N. Jarmie, M. W. McNaughton, and G. M. Hale (AIP, New York, 1981), p. 478.
[19]C. C. Foster, J. C. Collins, D. L. Friesel, W. W. Jacobs, W. P. Jones, M. D. Kaitchuck, P. Schwandt, and E. J. Stephenson (unpublished).
[20]H. Amakawa and K. Yazaki, Phys. Lett. 87B, 159 (1979).
[21]J. R. Wu, C. C. Chang, and H. D. Holmgren, Phys. Rev. C 19, 370 (1979).
[22]U. Bechstedt, H. Machner, G. Baur, R. Shyam, C. Alderliesten, O. Bousshid, A. Djaloeis, P. Jahn, C. Mayer-Böricke, F. Rösel, and D. Trautman, Nucl. Phys. A343, 221 (1980).